Hindered Coarsening of a Phase-Separating Microemulsion Due to Dispersed Colloidal Particles

Danielle D. van't Zand,[†,‡] Andrew B. Schofield,[†] Job H. J. Thijssen,[†,‡] and Paul S. Clegg[*,†,‡]

[†]School of Physics and Astronomy, [‡]Collaborative Optical Spectroscopy, Micromanipulation and Imaging Centre, University of Edinburgh, Edinburgh, EH9 3JZ, United Kingdom

ABSTRACT: The addition of sterically stabilized colloidal particles to a phase-separating microemulsion leads to dramatic changes in its demixing behavior, especially during the later stages. Our microemulsion is composed of reverse micelles of sodium dodecyl sulfate, pentanol, and water in a dodecane continuous phase which separates into micelle-rich and micelle-poor phases above a lower critical solution temperature. The poly(methyl methacrylate) particles preferentially partition into the less structured, micelle-poor phase. Nucleation of the minority phase or spinodal decomposition close to criticality continue to occur in the presence of particles, albeit with pronounced pretransitional clustering of particles when the micelle-poor phase is in the minority. The coalescence of micelle-poor droplets and the coarsening of micelle-rich domains are both strongly modified due to the presence of colloidal particles. We use our observations of the early stages of phase separation to understand these late stage changes.
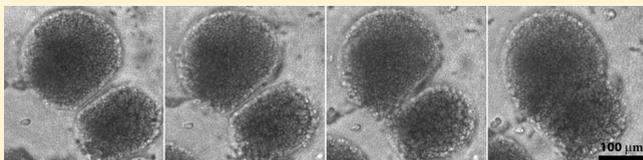
1. INTRODUCTION

Dispersing colloidal particles in a host solvent which itself has a phase transition has proved a productive starting point for creating novel soft materials. As the composite is induced to undergo a phase transition the host solvent tends to organize the particles although sometimes the particles can also disrupt the transition. Both the interaction between the particle and the solvent and the phase transition kinetics can be tuned to influence the outcome. Host solvents have included liquid crystals,[1−4] binary liquids[5−8] and polymer blends.[9−11] In the case of binary liquids novel soft solids have been created by tuning the particle surface chemistry so the particles either sequester to the liquid−liquid interfaces, to create a particle-stabilized emulsion[6] or a bijel[7] depending on the demixing kinetics, or partition into one of the domains, to create a different arrested medium.[12,13] Biliquid foams can also be created from particles in a binary liquid as the liquids remix.[14]

In many of these cases, phase separation of the host solvent occurs quickly and hence it is difficult to observe the behavior of the dispersed particles during demixing.[7,15] In this paper we use as our host solvent a system that phase separates slowly because it is a micellar fluid of carefully chosen composition; the transition can be imaged in real time using microscopy techniques. The solvent is a microemulsion which, in a certain composition range Figure 1, is found to behave in a manner analogous to a binary liquid mixture.[16] Upon warming the micelle−micelle interactions become increasingly attractive and the system phase separates into two microemulsions with different micelle concentrations, here referred to as the micellar 'gas' phase and micellar 'liquid' phase, which respectively contain a lower and higher concentration of micelles.[17] To this system we have added sterically stabilized colloidal particles made of poly(methyl methacrylate), PMMA. In the absence of micelles, these particles

interact via a short-range steric repulsion. The addition of a smaller species, e.g., micelles, to such a dispersion, as in ref 18 for charge-stabilized particles and worm-like micelles, can induce depletion attractions between the particles provided that the micelles are not adsorbed. Small, disordered clusters of PMMA particles are known to form in dispersions as the particles are made increasingly 'sticky' using depletion attraction or by other means.[19]

The interaction between sterically stabilized PMMA particles and a host dispersion of ionic surfactants has been explored for the case where the host does not phase separate.[20,21] The surfactant concentrations were sufficient for micelle formation but lower than those employed here (see section 2). The presence of micelles was found to be associated with charging of the colloidal particles. Due to the low dielectric constant of the host solvent this led to long-range repulsions between particles. Increasing the micelle concentration had a similar effect to adding salt to an aqueous colloidal suspension: the electrostatic repulsion was progressively screened while the zeta potential remained approximately constant. For the highest concentrations studied a short-range attraction was also observed.[20] Systematic study using anionic, cationic and nonionic surfactants led to a quantitative model of the competitive adsorption of both positively and negatively charged micelles.[21] In our system the particles may experience a change in micellar concentration as the microemulsion phase separates.

Even before phase separation we can expect changes to particle−particle interactions. Previously, induced clustering of colloidal particles has been studied as the binodal is approached
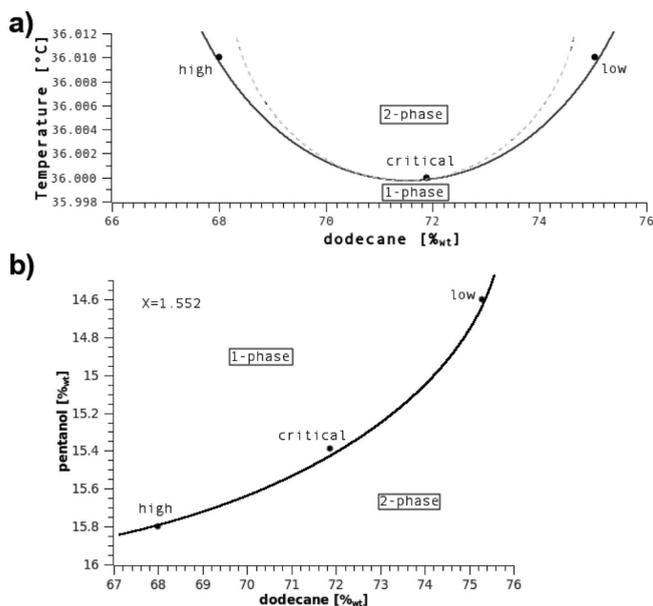
Figure 1. Sections of the phase diagram of the sodium dodecyl sulfate (SDS), water, pentanol, and dodecane system. Throughout the water/SDS ratio is 1.552. Precise compositions of the points 'high', 'critical', and 'low' are given in Table 1. (a) Phase behavior with temperature and dodecane concentration; the system is equivalent to partially miscible binary liquids with a lower critical solution temperature. (b) Phase behavior on varying both the pentanol and the dodecane concentrations.

Table 1. Microemulsion Compositions[a]

composition	dodecane (%)	pentanol (%)	water/SDS (%)
high	68.0	15.8	16.2
critical	71.87	15.39	12.74
low	75.3	14.6	10.2
dilute	83.0	14.0	3.0

[a] The compositions by mass of microemulsions used for these studies; throughout the water/SDS ratio is 1.552. The words 'high', 'low', and 'dilute' refer to the concentration of micelles; 'critical' is the composition for which the lower critical solution temperature is 36 °C.

Table 2. Microemulsion Properties in the Absence of PMMA[a]

microemulsion	diameter (nm)	density (g/cm^3)	$\sim\Phi_v$ micelles (%)
dilute	6.5 ± 0.2	0.759	5.5
before separation	75 ± 10	0.792	18
micellar liquid	54.1 ± 1.5	0.796	20
micellar gas	21.4 ± 0.3	0.785	16

[a] Sizes of (clusters of) micelles determined using DLS at $T = 25$ °C in the microemulsion. The 'dilute' system used for these studies has 83%$_w$ dodecane and may show the size of individual micelles. The microemulsion 'before phase separation' contains 68%$_w$ dodecane (corresponding to 'high' in Table 1) and shows the greatest extent of micelle clustering/coalescence. Micelles for the micellar-liquid and micellar-gas phases, following demixing of the 'high' sample above 36.01°C, were also characterized but only after re-cooling to $T = 25$ °C. The final column is an estimate of the volume fraction of micelles in each microemulsion.

from the mixed phase.[22−27] The behavior approaching the critical point has been studied more recently.[28] Both simple liquids, which are often mixtures of water and 2,6-lutidine,[22,23,26] and micellar fluids, nonionic surfactant micelles in water,[24,25] have been used as the host. Those using simple liquids have tended to view the particles as a small perturbation to a pseudobinary system.[26] The clustering behavior has been attributed to the appearance of a wetting layer as the binodal is approached although this is contested.[23] Observations of particles in phase-separating micellar solvents have been interpreted as a ternary system; the water is considered to partition between a particle-rich phase and a micelle-rich phase.[25] In all these systems the particles are charge stabilized and pronounced clustering of particles is observed when the phase favoring the particles is in the minority. This phenomenon is of interest here as, if it also occurs for our sterically stabilized PMMA particles, it will influence demixing as the binodal is crossed.

As shown in section 3, one of our central observations is the slow coarsening of domains following phase separation. Detailed studies have been carried out on the slow evolution of dynamically asymmetric domains, e.g., a polymer solution, in which the polymer-rich phase is much more viscous than the solvent-rich phase.[29] In such systems the flow properties play an important role in determining the kinetic pathway for demixing. For near-critical compositions, demixing initially occurs via the nucleation of solvent-rich holes, which form the minority phase. As these droplets grow in time, the polymer-rich phase becomes network-like, the pattern being dominated by the elastic force-balance condition. During this intermediate stage, the system undergoes a phase inversion, i.e., the volume of the polymer-rich phase keeps decreasing with time and ends up as the minority phase, which has been suggested to be a unique feature of viscoelastic phase separation. When samples for which the polymer-rich

phase is in the minority are quenched, a moving droplet phase can be observed. On phase separation polymer-rich nuclei form which bounce off each other rather than coalescing on contact. Separately, in the context of emulsion science, the very slow coalescence of highly viscous bitumen droplets has been investigated[30] with the bulk behavior compared to a model of viscous sintering.

Here we present clear observations of the particle behavior during each stage of microemulsion phase separation. This begins, section 3.1, with pronounced pretransitional clustering when the micelle-poor phase is in the minority. Following heterogeneous nucleation these clusters can evolve into colloidal 'comets'. We also present, section 3.2, droplets that do not readily coalesce and, section 3.3, slowly coarsening network-like regions leading to bizarre biliquid foams comprised of microemulsions. We conclude, section 4, that even at low volume fraction, the particles have strongly modified the flow properties of the microemulsion.

2. MATERIALS AND METHODS

Dodecane (Acros Organics, 99%), pentanol (Fisher Scientific, >98%), sodium dodecyl sulfate (SDS, Acros Organics, 99% for biochem.), and water (Fisher Scientific, HPLC grade) were used as received. Microemulsion samples were prepared by weight with compositions indicated in Table 1. In all the samples the water/SDS ratio is kept constant at 1.552;[31] for the composition used the lower critical solution temperature is 36 °C. The sizes of the micelles in microemulsions of different composition in the absence of colloids were measured using dynamic light scattering (DLS) with 514 nm light (Ar-ion laser), and scattered light measured at an angle of 20°; see Table 2.
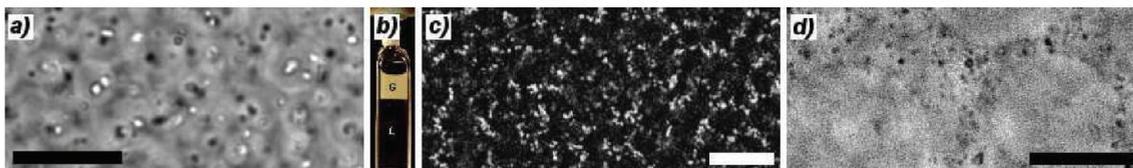
Figure 2. Showing that the phase transition behavior of the microemulsion persists when PMMA particles ($0.05\%_w$) are added and the samples warmed at 0.1 °C/min into the two-phase region (∼36 °C, Figure 1); compositions from Table 1 (a,b) high, (c) critical, (d) low. (a) Bright-field micrograph of micelle-poor phase nuclei containing PMMA particles. (b) PMMA particles (yellow) partition into the micelle-poor phase. Cuvette 1 cm wide. (c) Confocal micrograph of spinodal decomposition in the presence of PMMA particles (white). (d) Bright-field micrograph of micelle-rich phase droplets with PMMA particles in the continuous phase. Scale bars 50 μm.

Polyhydroxystearic acid (PHS) stabilized poly(methyl methacrylate) (PMMA) colloids were synthesized in Edinburgh. The particles (radius 530 nm, polydispersity 20%, DLS) were fluorescently labeled using 7-nitrobenzo-2-oxa-1,3-diazol-4-yl (NBD, CAS 10199−89−0). Prior to dispersion the colloids were washed 6 times using hexane and dried at 60 °C under vacuum for at least six hours to minimize residual hexane.

Once the PMMA particles were dispersed in the microemulsion a measurement of the potential for the particle at its Stern layer, i.e., the zeta potential, was used to confirm that the micelles cause the particles to become charged in keeping with refs [20,21]. Using a Zetasizer Nano we find for $0.1\%_w$ PMMA in the dilute microemulsion (Table 1) $\zeta \approx 30$ mV. For higher concentrations of micelles the spread of zeta potential values measured became extremely broad.

The phase behavior was studied under controlled temperature with warming always at 0.1 °C/min (Linkam Scientific LTS350) using bright-field microscopy (Olympus BX50), with a 20×, NA 0.40 objective. Samples were transferred into glass cuvettes (Starna) using a pasteur pipet and, prior to study, rehomogenized using a vortex mixer. Particles and micelles were imaged separately but simultaneously via fluorescence confocal microscopy, using 20×, NA 0.45 objective. A Nikon E800 upright microscope was used in conjunction with the Biorad Radiance 2100 scanner operating an Ar-ion laser, 488 nm, and a diode laser, 637 nm. The water in the micelles was fluorescently labeled using a small quantity (<0.001 g) oxazine 170 perchlorate (Sigma Aldrich 95%, CAS 62669−60−7) when required. The images of fluorescent micelles in the bottom row of Figure 4 underwent digital post processing with a bandpass filter and with contrast stretching for clarity.

3. RESULTS AND DISCUSSION

On warming, the micelle−micelle interactions become increasingly attractive leading to phase separation; there is an associated change in effective micelle size and the possibility of a change in the interaction between PMMA particles. Figure 2 shows that, qualitatively, the phase transition behavior of the microemulsion persists when a low concentration of PMMA particles is added (e.g., $\phi = 0.05\%_w$) and the sample is warmed at 0.1 °C/min into the two-fluid regime. At high-micelle concentration (Figure 2a), the micelle-poor phase nucleates around the colloids, while at low-micelle concentration the micelle-rich nucleates with the colloids remaining in the continuous phase (Figure 2d). For low particle concentrations, on both sides of the phase diagram, the nucleated droplets coalesce on contact and ultimately the particles are entrained within the micelle poor-phase as it rises (Figure 2b). For samples of critical composition (Figure 2c) spinodal decomposition continues to be observed.[32]

3.1. Pretransitional Clustering of Particles and 'Comet' Formation. As the concentration of particles is increased from $0.1\%_w$ to $0.25\%_w$ pretransitional clustering becomes prominent at high-micelle concentration (Figure 3). It can be seen that the colloids begin to form irregularly shaped clusters on warming

(Figure 3, 1). These clusters then further aggregate (Figure 3, 2) and subsequently acquire a transparent surface layer (Figure 3, 3), which indicates that heterogeneous nucleation of the micelle-poor phase occurred as the binodal was crossed. The two-fluid regime is entered between the third and fourth images of the sequence. When the temperature is sufficiently high the colloids redisperse within the micelle-poor phase droplet (Figure 3, 4), the clusters lose their irregular shape and become increasingly spherical. At this composition droplets containing dispersed colloids coalesce on contact (Figure 3, 5). Figure 4 is a time sequence taken using fluorescence confocal microscopy with the micelles dyed; here we can see that the colloidal clusters appear to be associated with low concentrations of micelles both in clusters and subsequently in the micelle-poor phase droplets.

Once the clusters have redispersed (Figure 3, 4) within a micelle-poor phase droplet, in a high-micelle concentration sample, new behavior emerges driven by gravity. Figure 5 shows that as the buoyant micelle-poor phase droplets rise particles can be left behind. The resulting droplets with a trail of particles resemble 'comets'. That the particles easily fall out of the cluster inside the micelle-poor phase droplet indicates that they are loosely bound to each other and also that the energy cost of having a particle in the more structured phase is a surmountable barrier. The similarity of the micellar-gas and liquid phases of the host microemulsion is evidenced by the very low interfacial tension ($\sim 10^{-2}$ mN/m[33]). From our results we cannot tell whether a small quantity of micellar-gas phase is entrained with the particles as they fall. It is possible to very roughly estimate the size of a particle cluster that is required to break through an interface based on the idea of a gravitational capillary length.[34] Here we take the density difference between the PMMA particles (1180 kg m^{-3}) and the continuous phase (796 kg m^{-3}) but the interfacial tension between the micellar-gas and micellar liquid phases (above). This suggests that the particle clusters that fall from the comets should be around 50 μm in size; a little larger than actually seen, Figure 5.

In the high-micelle concentration regime, we observe pretransitional particle clustering, heterogeneous nucleation of micelle-poor phase droplets and subsequent redispersal of the particles within these droplets, Figure 3 and schematically in Figure 6 (a−c). By considering this process and the subsequent formation of colloidal 'comets' we can begin to understand the interactions between PMMA particles. Prior to phase separation we note, consistent with refs 20,21 that the particles may have acquired charge due to adsorbed micelles. Hence the PMMA particles may tend to repel one another electrostatically. In spite of this we also observe strong pretransitional clustering of these particles in samples in the high-micelle concentration regime. We believe that the pretransitional clustering is not due to a depletion
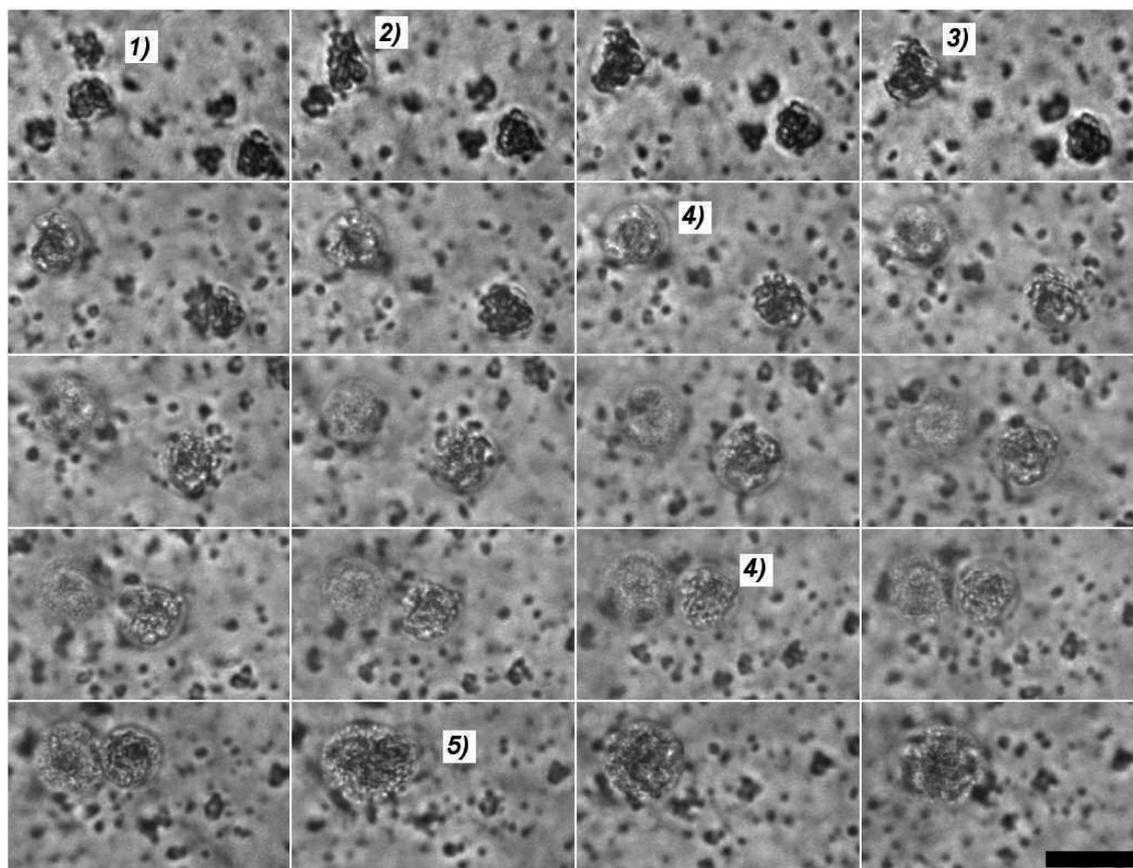
Figure 3. Showing the stages of PMMA particle $(0.25\%_w)$ clustering when the micelle-poor phase is in the minority and the sample is warmed at 0.1 °C/min (Table 1, composition 'high'). The sequence begins in the top left at 35.98 °C and finishes at bottom right at 36.17 °C with 6 s between frames. The binodal is crossed between the third and fourth frames. Scale bar 50 μm. The numbers are referred to in the text.
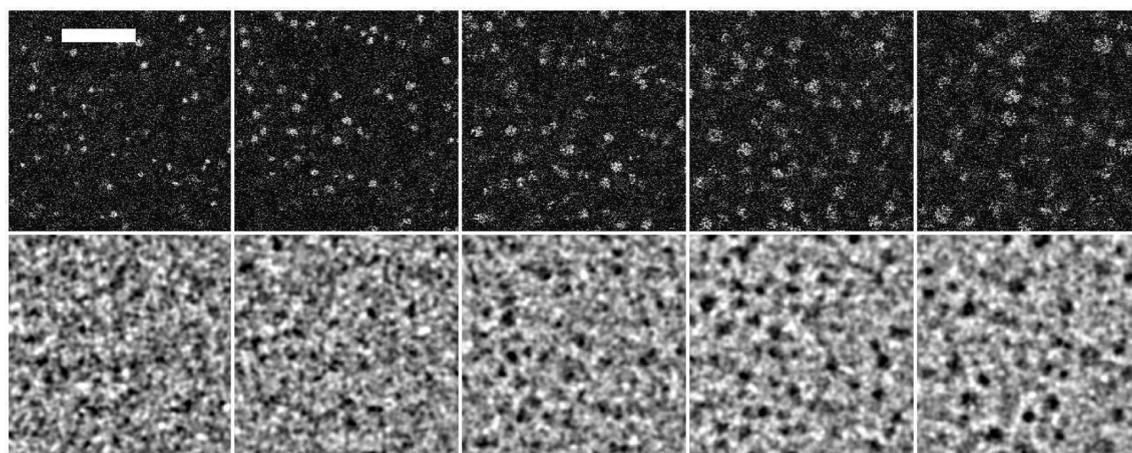

Figure 4. Time series of confocal images beginning on the left at 35.81 °C; images separated by 1 min as the sample is warmed at 0.1 °C/min. The top row shows the colloidal particles and the bottom row shows the micelles following postprocessing of images. Small differences in matching frames can be expected due to slight focal-plane mismatches between 488 and 637 nm excitations. Composition: Table 1, high with $2\%_w$ of PMMA. Scale bar 50 μm.

attraction, in contrast to the type of cluster formation studied in ref 19 because of the strong dependence on the composition of the host microemulsion. Going from 'high' to 'critical' (Table 1) is sufficient to switch off clustering—suggesting that it is related to the binary-liquid phase behavior. Typically, such pretransitional

particle clustering in a binary liquid host is most pronounced on the side of the phase diagram for which the minority phase preferentially wets the particle surface.[26] In the high-micelle concentration regime the minority phase is the micelle-poor phase. Consistent with this, we find that in all of our experiments, for samples of all compositions,
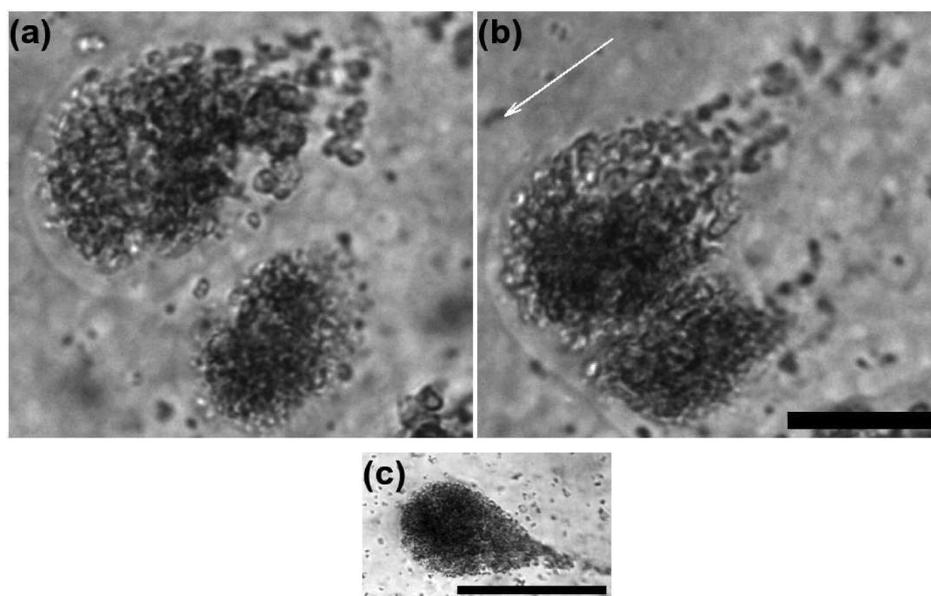
Figure 5. Typical colloidal *comets* imaged using bright-field microscopy after the sample has been warmed at 0.1 °C/min to 36.5 °C. Arrow in (b) shows the direction of travel. The PMMA particles (a,b) 0.15%$_w$, (c) 0.5%$_w$ and clusters are falling out of a micelle-poor phase bubble as it rises to the top. Sample composition: Table 1, high. Scale bars (a,b) 50 μm; (c) 100 μm.
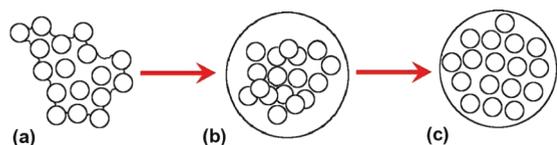

Figure 6. (a) Showing the particle clustering due to a wetting layer that is likely to be dodecane; (b) heterogeneous nucleation of a droplet, likely to include micelles, onto the cluster does not cause immediate redispersal; (c) subsequent redispersal of particles within the droplet. These cartoons can be compared with observations in Figures 3 and 4.

the particles preferentially partition into the micelle-poor phase (e.g., Figure 2b). Up to this point the pretransitional clustering behavior appears to follow the pattern observed by Beysens and others.[26]

Further observations demonstrate that this understanding may need to be refined. First, we find that when heterogeneous nucleation occurs the PMMA particles initially remain clustered; they only redisperse to fill the whole nuclei volume after a delay. This process is pictured schematically in Figure 6. Second, our fluorescence studies suggest that there are relatively few micelles within the micelle-poor phase droplets when compared with the micelle-rich continuous phase (Figure 4 and Figure 7f). By contrast the micellar-gas phase, characteristic of pure microemulsion, is expected to contain a high proportion of micelles albeit less than the micellar-liquid phase, see Table 2. We suggest that the pretransitional wetting layer, that drives clustering Figure 6-(a), is rich in dodecane and may contain few or no micelles. The subsequent nuclei that forms around the cluster is of the micellar-gas phase although this too may be characterized by a reduced population of micelles as indicated by our fluorescence results. Based on this we can understand the transition from clusters to dispersed particles inside the droplets: initially a depletion attraction exists between the PMMA particles which are coated with dodecane but have a cluster surface that is in contact with the micelles, Figure 6(b). As the dodecane from the particle

surfaces and the micellar-gas phase diffuse, mix and equilibrate this attraction diminishes. Ultimately the particles unstick as the depletion attraction becomes negligible, Figure 6(c). An additional role may be played by electrostatic repulsion due to any micelles adsorbed on the particles. The subsequent 'comet' sightings (Figure 5) clearly demonstrate that the particles in the droplets are scarcely attracting each other.

While the warming rate was kept at 0.1 °C/min for all experiments presented here preliminary studies suggest that warming at a significantly faster rate suppresses both the pretransitional clustering and comet formation. In the case of pretransitional clustering this is likely to be due to the reduced time for particles to encounter each other.

3.2. Hindered Coalescence of Micelle-Poor Phase Droplets Due to Particles. Figure 7(a−d) shows a time sequence of two particle-filled droplets during coalescence. The coalescence proceeds remarkably slowly; even when the droplets are in repeated contact they do not coalesce immediately. Another notable feature is the flat regions on each droplet. When the droplets finally begin to coalesce, it can be seen that a bridge forms between them through which material flows (Figure 7 c). The bridge becomes wider and coalescence then occurs easily (Figure 7 d). In this system particles are not observed to be located on interfaces during phase separation at any stage. This is in contrast to many liquid−liquid systems with higher interfacial tension, where particles are trapped on the interfaces.[5,35] In an effort to determine whether a protective barrier of micelle-rich phase is trapped between droplets, fluorescence confocal microscopy was carried out with dyed micelles, (Figure 7 e−g). There appears to be little to prevent the droplets coalescing.

Our results suggest that slow coalescence of particle-filled droplets is unlikely to be due to a layer of micelle-rich phase, Figure 7(e−g). In addition, the particle-filled droplets acquire a long-lived deformation in preference to coalescing when they are in repeated contact. There is no interfacial layer of colloidal particles and the failure to coalesce quickly appears to be associated with the contents of the droplet not with the interface.
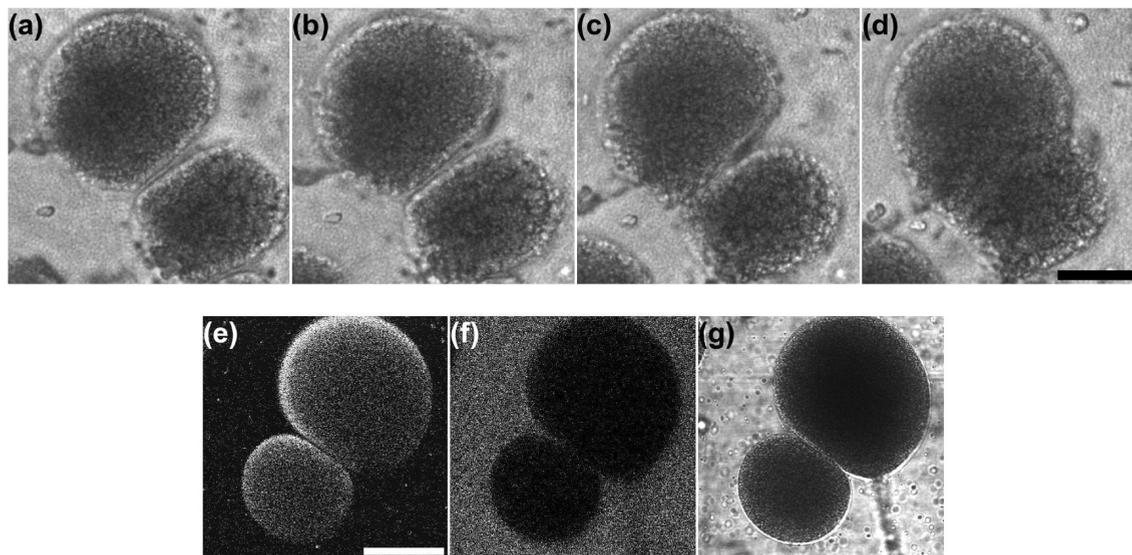
Figure 7. Showing that particle filled droplets only coalesce extremely slowly. Composition: Table 1, high with 0.5%$_w$ PMMA particles. (a–d) A time sequence beginning on the left at 36.5 °C with 12 s between frames as the sample is warmed at 0.1 °C/min. In total these droplets made contact repeatedly for 3–4 min prior to coalescence. (e–g) Micrographs showing fluorescence from (e) colloidal particles, (f) micelles and (g) bright-field image respectively. Scale bars 100 μm.
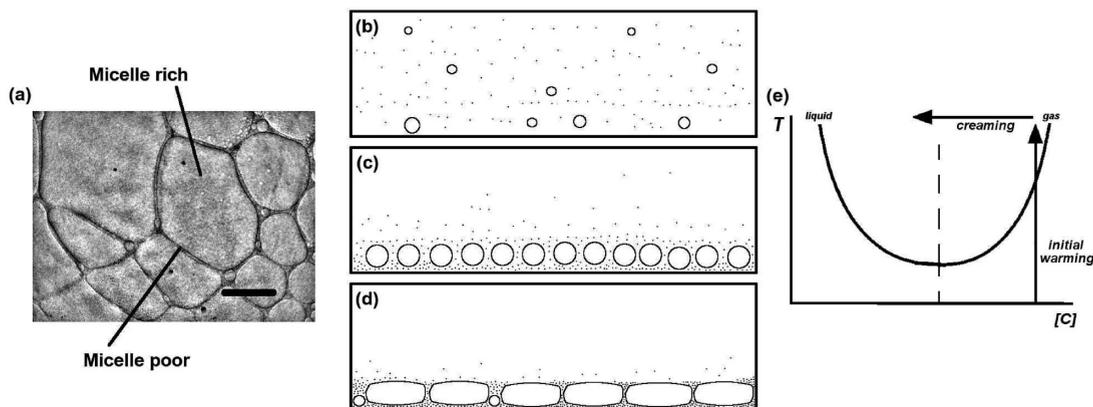

Figure 8. (a) An extraordinary liquid–liquid foam comprised of micelle-rich domains that are nonspherical in a micelle-poor continuous phase formed after warming at 0.1 °C/min to 37 °C. Composition: Table 1, low; with 0.1%$_w$ of PMMA particles. Scale bar 200 μm. (b–d) Suggested vertical stratification of the sample as the micelle-rich phase droplets grow. Open shapes represent micelle-rich domains; dots represent PMMA particles. (e) Change in local composition at the base of the sample indicated in relation to the binodal line.

From the long-lived deformations we conclude that the contents of the droplet reorganizes only very slowly. The droplet may have a yield stress or be viscoelastic; at the very least it is highly viscous. The slow reorganization of the droplets will retard coalescence. Such behavior has been observed before in the 'moving droplet phase' of viscoelastic phase separation[29] and in the viscous sintering of bitumen emulsions.[30] We can obtain an estimate of the effective viscosity of the particle-filled droplet: the relaxation time $\tau_R \sim \eta d/\gamma$. Here $\tau_R \approx 240$ s, $d \approx 200\ \mu$m and $\gamma \approx 10^{-5}$ Nm^{1-}. This gives $\eta \approx 10$ Pas, 4 orders of magnitude higher than dodecane.

3.3. Microemulsion Biliquid Foam. Figure 8(a) shows the late stage behavior when the micelle-rich phase is in the minority (Table 1, low-micelle concentration). A very important point is that, from a two-dimensional image, it appears that the domains of micelle-rich phase are not the minority phase. Initially micelle-rich droplets and colloidal particles are homogeneously distributed within the micelle-poor continuous phase. The micelle-rich droplets coalesce on contact and both they and the particles are ultimately observed in abundance at the base of the cell. Similar behavior has been studied before in the case of creaming droplets stabilized by interfacial-particles in a continuous phase rich in those particles.[14] In both our system and that one the composition of the system changes locally. Here the micelle-rich phase droplets and the colloidal particles are dense and tend to sediment (shown schematically in Figure 8 b–d). The base of the cell becomes a novel biliquid foam comprised of micelle-rich phase and the micelle-poor phase which contains the particles. The micelle-rich phase becomes the majority phase - but only locally, Figure 8(e).

Figure 9 shows that, once ruptured, the continuous phase of the biliquid foam takes more than five seconds to retract.
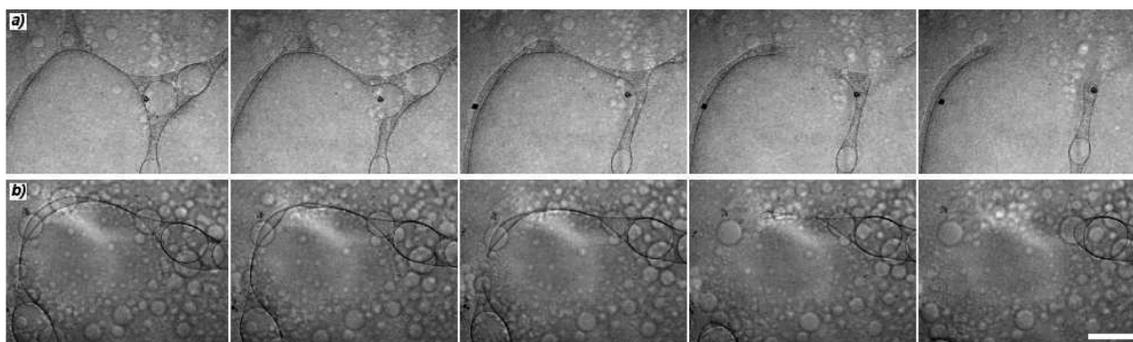
Figure 9. Two bright-field microscopy time sequences both beginning on the left at 37 °C showing the slow aging of the biliquid-foam; 2 s between frames with warming at 0.1 °C/min. Composition: Table 1, low; with 0.1%$_w$ of particles. As domain walls, comprised of micelle-poor phase and PMMA particles, rupture they retract only slowly. Scale bar 100 μm.

Also observable is the bulging of the interfaces which is akin to the dimple formation encountered in foam film drainage.[36,37] The domain boundaries are comprised of the particle-containing micelle-poor phase which hinders the coalescence of the micelle-rich phase domains. The boundaries have become a viscoelastic medium due to the presence of the PMMA particles. This effect appears for particle volume fractions above 0.1%$_w$. A significant volume fraction of repulsive particles gives rise to the elastic boundary regions that are slow to reorganize leading to the slow retraction exhibited following the coalescence between two domains (Figure 9).

While the warming rate was kept at 0.1 °C/min for all experiments presented here preliminary studies suggest that the biliquid foam does not form when the warming rate is significantly increased. This might be a result of the reduced time available for the micellar-rich domains and the PMMA particles to sediment under gravity.

4. CONCLUSIONS

We have presented the first study of sterically stabilized colloidal particles in a phase-separating microemulsion. We have shown that for low concentrations of particles the demixing behavior is preserved with novel changes only occurring as more particles are added. In all regimes the particles tend to partition into a phase containing fewer micelles. We have shown the pretransitional particle clustering and subsequent nucleation and redispersal within the droplet when the sample is in the high micelle-concentration regime. Once redispersed the particles can fall out of the droplets and hence begin to resemble a colloidal 'comet'. In the late stage, for both high and low concentrations of micelles, coalescence of the minority domains is surprisingly slow. This leads to a curious microemulsion biliquid foam for the low concentration case.

By considering the interactions between the colloidal particles as a function of the volume fraction of micelles we have been able to understand, at least qualitatively, the hindered coarsening behavior. On both sides of the phase diagram we have observed a significant slow down in coarsening behavior due to the addition of particles. This is observed as very slow coalescence of particle-filled micellar-gas phase droplets and slow coarsening of microemulsion biliquid foams. We suggest that the particle-filled micellar-gas phase has become extremely viscous even for the very low volume fractions used here. This is a consequence of the effective interactions between the particles induced by the

medium. Electrostatic charges due to micelles adsorbed on the particles may be decisive.

■ AUTHOR INFORMATION

Corresponding Author
*E-mail: paul.clegg@ed.ac.uk.

■ REFERENCES

(1) Meeker, S. P.; Poon, W. C. K.; Crain, J.; Terentjev, E. M. *Phys. Rev. E* **2000**, *61*, R6083–R6086.

(2) Anderson, V. J.; Terentjev, E. M.; Meeker, S. P.; Crain, J.; Poon, W. C. K. *Eur. Phys. J. E* **2001**, *4*, 11–20.

(3) Sharma, K. P.; Kumaraswamy, G.; Ly, I.; Mondain-Monval, O. *J. Phys. Chem. B* **2009**, *113*, 3423–3430.

(4) Sharma, K. P.; Ganai, A. K.; Sen Gupta, S.; Kumaraswamy, G. *Chem. Mater.* **2011**, *23*, 1448–1455.

(5) Gallagher, P. D.; Maher, J. V. *Phys. Rev. A* **1992**, *46*, 2012–2021.

(6) Clegg, P. S.; Herzig, E. M.; Schofield, A. B.; Egelhaaf, S. U.; Horozov, T. S.; Binks, B. P.; Cates, M. E.; Poon, W. C. K. *Langmuir* **2007**, *23*, 5984–5994.

(7) Cates, M. E.; Clegg, P. S. *Soft Matter* **2008**, *4*, 2132–2138.

(8) Lee, M. N.; Mohraz, A. *Adv. Mater.* **2010**, *22*, 4836–4841.

(9) Chung, H.-J.; Ohno, K.; Fukuda, T.; Composto, R. J. *Nano Lett.* **2005**, *5*, 1878–1882.

(10) Si, M.; Araki, T.; Ade, H.; Kilcoyne, A. L. D.; Fisher, R.; Sokolov, J. C.; Rafailovich, M. H. *Macromolecules* **2006**, *39*, 4793–4801.

(11) Firoozmand, H.; Murray, B. S.; Dickinson, E. *Langmuir* **2009**, *25*, 1300–1305.

(12) Tanaka, H. *J. Phys.: Condens. Matter* **2001**, *13*, 4637–4674.

(13) Li, L.; Miesch, C.; Sudeep, P. K.; Balazs, A. C.; Emrick, T.; Russell, T. P.; Hayward, R. C. *Nano Lett.* **2011**, *11*, 1997–2003.

(14) Thijssen, J. H. J.; Clegg, P. S. *Soft Matter* **2010**, *6*, 1182–1190.

(15) Thijssen, J. H. J.; Clegg, P. S. *J. Phys.: Condens. Matter* **2010**, *22*, 455102.

(16) Roux, D. *J. Phys. (Paris)* **1986**, *47*, 733–738.

(17) Roux, D.; Bellocq, A. M.; Leblanc, M. S. *Chem. Phys. Lett.* **1983**, *94*, 156–161.

(18) Petekidis, G.; Galloway, L. A.; Egelhaaf, S. U.; Cates, M. E.; Poon, W. C. K. *Langmuir* **2002**, *18*, 4248–4257.

(19) Stradner, A.; Sedgwick, H.; Cardinaux, F.; Poon, W. C. K.; Egelhaaf, S. U.; Schurtenberger, P. *Nature* **2004**, *432*, 492–495.

(20) Hsu, M. F.; Dufresne, E. R.; Weitz, D. A. *Langmuir* **2005**, *21* 4881–4887.

(21) Roberts, G. S.; Sanchez, R.; Kemp, R.; Wood, T.; Bartlett, P. *Langmuir* **2008**, *24*, 6530–6541.

(22) Beysens, D.; Estéve, D. *Phys. Rev. Lett.* **1985**, *54*, 2123–2126.

(23) Gallagher, P. D.; Kurnaz, M. L.; Maher, J. V. *Phys. Rev. A* **1992**, *46*, 7750–7755.

(24) Koehler, R. D.; Kaler, E. W. *Langmuir* **1997**, *13*, 2463–2470.

(25) Jayalakshmi, Y.; Kaler, E. W. *Phys. Rev. Lett.* **1997**, *78*, 1379–1382.

(26) Beysens, D.; Narayanan, T. *J. Stat. Phys.* **1999**, *95*, 997–1008.

(27) Lu, X. H.; Mochrie, S. G. J.; Narayanan, S.; Sandy, A. R.; Sprung, M. *Phys. Rev. Lett.* **2008**, *100*, 045701.

(28) Hertlein, C.; Helden, L.; Gambassi, A.; Dietrich, S.; Bechinger, C. *Nature* **2008**, *451*, 172–175.

(29) Tanaka, H. *J. Phys.: Condens. Matter* **2000**, *12*, R207–R264.

(30) Philip, J.; Bonakdar, L.; Poulin, P.; Bibette, J.; Leal-Calderon, F. *Phys. Rev. Lett.* **2000**, *84*, 2018–2021.

(31) Roux, D.; Bellocq, A. M. *Phys. Rev. Lett.* **1984**, *52*, 1895–1898.

(32) van 't Zand, D. D. *Particles in Complex Fluids*; Ph.D. Thesis; University of Edinburgh, Edinburgh, U.K., 2010.

(33) Bellocq, A. M.; Gazeau, D. *J. Phys. Chem.* **1990**, *94*, 8933–8938.

(34) Tavacoli, J. W.; Thijssen, J. H. J.; Clegg, P. S. *Soft Matter* **2011**, *7*, 7969–7972.

(35) Binks, B. P.; Horozov, T. S. *Colloidal Particles at Liquid Interfaces*, CUP, 2006; Chapter 1, pp 1–74.

(36) Joye, J.-L.; Miller, C. A.; Hirasaki, G. J. *Langmuir* **1992**, *8*, 3083–3092.

(37) Exerowa, D.; Kruglyakov, P. M. *Foam and Foam Films*; Elsevier, 1998.